Available online at www.sciencedirect.com

ScienceDirect

Procedia Engineering 99 (2015) 1548 – 1560

Procedia Engineering

www.elsevier.com/locate/procedia

"APISAT2014", 2014 Asia-Pacific International Symposium on Aerospace Technology, APISAT2014

Experimental Study of Surge and Rotating Stall Occurring in High-speed Multistage Axial Compressor

Changzheng LI*, Siqi XU, Zhiqi HU

Northwestern Polytechnical University, POB631, West Youyi Road 127, Xi'an 710072, China

Abstract

The analysis of signals of surges and rotating stalls occurring and processing is essential to reveal the characteristics of instability phenomena, to develop detecting methodology and active control technique, to assure the rig and compressor safety. A high-speed 7-stage compressor was tested on a rig, with 10 channels of casing static pressures and a channel of outlet total pressure. It illustrates by the case with the rotating speed 16,400RPM. Firstly, to detect the stall precursors, the spectrum analysis and the short-time-Fourier-transform (STFT) are employed. It shows the precursors are formed about 3.5s before the surge point in each stage individually. Then, the correlation functions are calculated to analysis the relationship between casing static pressures. Results show that the rotating stalls of the 1-3stages have phase differences, while the 4-7stages do not. Finally, the time-domain waveforms analysis instruct that the stagnation cell of surge is firstly formed between the 3rd and the 4th stator rows, and then moves downwards. The surge is companied with the rotating stalls. The front 3 stages are in the cycles of the stall-surge-recover-stall in the whole surge process.

Peer-review under responsibility of Chinese Society of Aeronautics and Astronautics (CSAA)

Keywords: Surge; Stall; Aerodynamic installbilty; Signal processing; Compressor.

1. Introduction

Stall and surge is a key point in the field of turbomachinery. The rotating stall degrades the performance of a compressor, while the surge may destroy the structure in few seconds. It is essential to discovery the mechanism, to

* Corresponding author. Tel.: +0-86-137-0023-3782.
E-mail address: lichangzheng@nwpu.edu.cn

Peer-review under responsibility of Chinese Society of Aeronautics and Astronautics (CSAA)
doi:10.1016/j.proeng.2014.12.707

enlarge the stable working range, to active control, and to ensure the safety of the machine, by experimental and data simulation study the aerodynamic instability phenomena.

In Ref [1], a 3.5 stage high speed compressor (rotating speed: 11,543 RPM) was studied. Four frequencies, about 9-12 times of rotating frequency, linked to rotating stall. Then, an antisurge active control system based on the detecting of the frequencies has been designed. In Ref [2], simulations and experiments of University of Cambridge and MIT tried to explain the dynamic flow nature of spike-type rotating stall of low-speed single stage compressors. It can be seen from figures that rotating stalls make regulated fluctuations of pressures. The circumferential located sensors get different phases which connected to angles and rotating speed. In Ref [3], a six-stage axial flow compressor was studied. Conclusions were drawn from the stage characteristics that at 60% and 80% full speed, the front stages of the compressor entered the unstable flow conditions before the downstream stages. The axial casing pressure traces increased where there was a stall cell, followed by a sharp decreased waveform. The circumferential pressure traces had different phase which connected with the circumferential locations. In Ref [4], an eight-stage compressor was studied with measure stations placed in the stage gaps. The stall precursors were detected when the Lyapunov exponents reach to zero. The first stall stage was confirmed by calculating the Lyapunov exponent of each axial pressure. In Ref. [5], the low-bypass twin-spool turbofan engine Larzac 04 was examined. A bypass throttling device was installed to force the low-pressure compressor into unstable situation. In the instability onset process, the signals of 5 sensors arranged circumferentially at the inlet upstream of the rotors leading edge had different phases, which instructed a spike type of stall precursor. In Ref. [6], the same result can be drawn with circumferential located pressures of spike-type stall precursors. In Ref. [7], the methods such as time series, spatial Fourier decomposition, traveling wave energy, and wavelet transform were used to depict the characteristics of the unsteady flow in axial compressors during pre-stall and stall inception.

In this paper, we focused on the dynamic pressures trace of a high-speed 7-stage compressor, tried to reveal the relationship of multi-sensor features and the propagation of the aerodynamic instability.

2. Experimental setup and instrumentation

The measurement was taken on a compressor rig with a 7-stage compressor. 10 static pressure and 1 total pressure stations are settled on the compressor, which are located as Fig.1. The pressure signals are named as “PABCCCD”. Here, the “P” stands for “Pressure”. The “A” is a number of stages. The “B” can be replace with “R” standing for the output of rotor, or “S” standing for the output of stator. The “CCC” means the circumferential angle of the measurement station. The “D” is replaced with “S” standing for the static pressure or “T” standing for the total pressure. All static pressures are measured with the casing static holes. The Kulite pressure sensors with high frequency response are used on all measurement stations. A high-speed data acquisition system is employed to record the signals of pressure and rotor speed. The simple rate is settled at 10 kHz.

The sketch of the test rig is shown in Fig. 2. In the testing program, firstly, keep the rotor speed steady. Secondly, push the compressor to the surge line by turning down the throttle slowly. Thirdly, turn up the throttle fast, and turn down the rotor speed as soon as surges appear. Finally, adjust the compressor to a steady working state. In this way, a group of aerodynamic install signals can be collected[8].

3. Methods

Usually, the Fourier transform is employed to analysis the spectral components of signals, to detect the stall or surge frequencies. It is a whole waveform transform to the frequency domain, i.e. there is no time information after transformation. When we try to find the beginning time of stall or surge, not only the frequencies but also the time information are needed. So, the short-time-Fourier transform is introduced (Equation 1).

$$STFT_x(t,\omega) = \int_{-\infty}^{\infty} x(\tau)h(\tau - t)e^{-j\omega\tau}d\tau \tag{1}$$

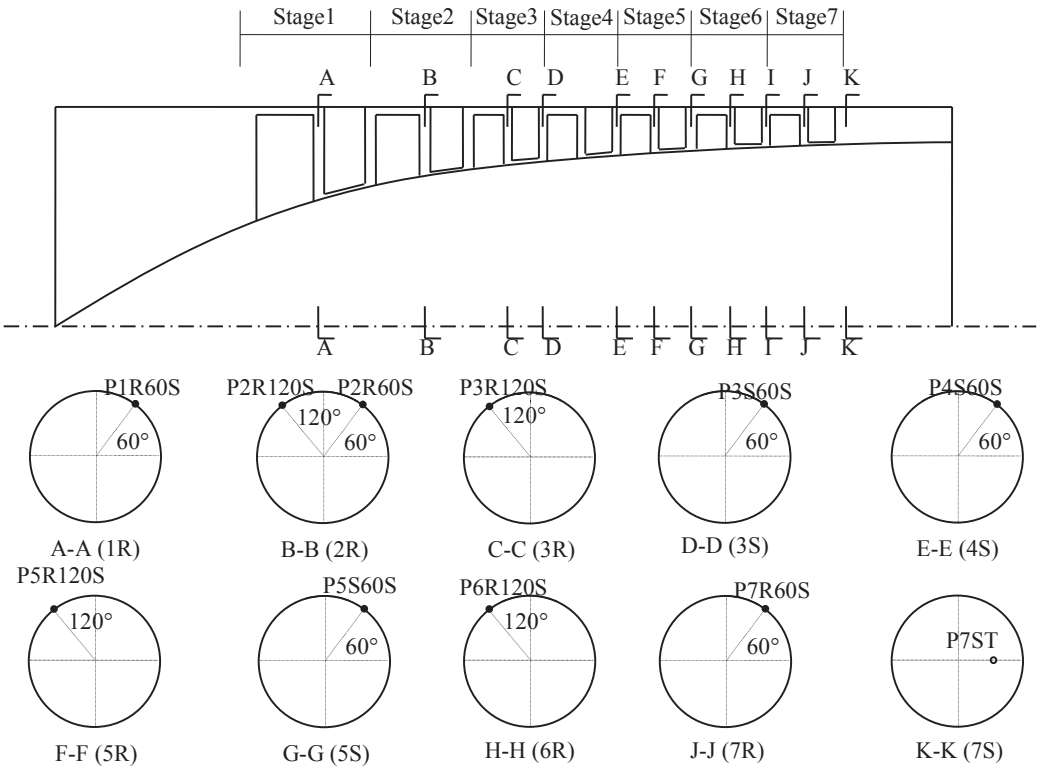

Fig. 1. Sketch of pressure measurement stations.

The correlation analysis is also used in this paper to calculate the periods or delay time of signals. The correlation function is defined by equation 2, while the normalized correlation function named correlation coefficient function is defined by Equation 3.

$$R_{xy}(m)=\frac{1}{N-|m|}\sum_{k=0}^{N-|m|-1}x(k+m)y(k) \tag{2}$$

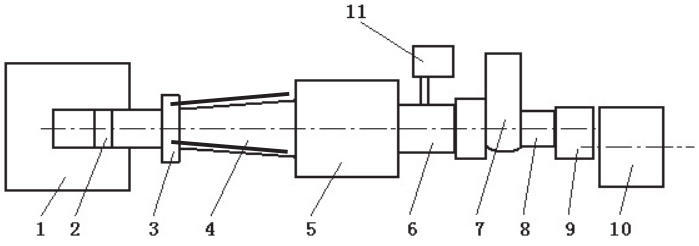

1 dust screen
2 flow measure device
3 air inlet shutter
4 intake diffuser
5 pressurizingtank
6 test piece
7 exhaust section
8 torquemeter
9 gearbox
10 power unit
11 bleed system

Fig. 2. Sketch map of axis-compressor test rig.

$$\rho_{xy}(m) = \frac{R_{xy}(m)}{\sigma_x \sigma_y} \tag{3}$$

4. Experimental results and discussion

4.1. Experimental results

The signals of fluctuant pressures through the aerodynamic instability test are shown in Fig.3, while the rotor speed is 16,400 rpm.

It can be read from Fig.3 that the throttle valve was closing down during 0-1s. Then, the throttle valve was closing down gradually from 5s until about 9.300s, namely 2525.6 rotor revolutions, when the compressor went into the surge state.

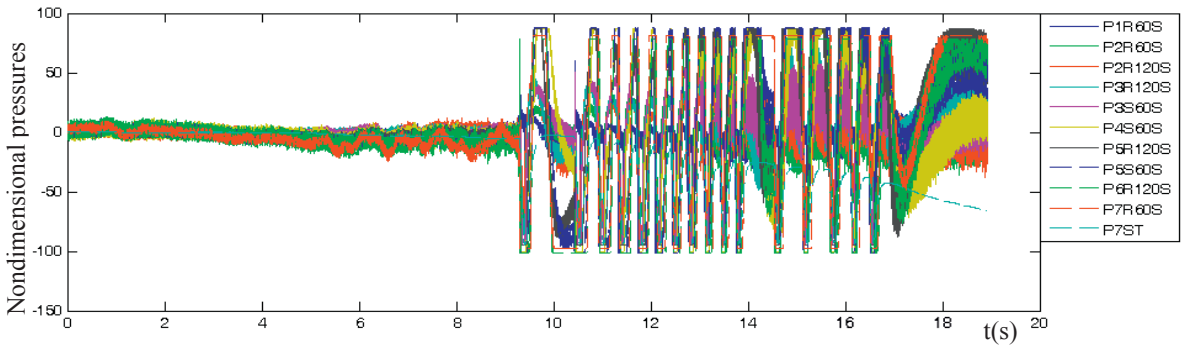

Fig. 3. Pressure signals of instability process

4.2. Compressor stall process

The compressor works at a high speed, as 16,400 rpm or 273.3Hz. About 36 data can be collected in a rotor revolution, when the sampling frequency is 10 kHz. In this way, the spike precursors which occupy only one to several blade passages are difficult to be detected, because the anti-alias filters before analog/digital converters smooth the uneven pressure of the blade passages. It seems that the compressor always goes into instability state with a modal wave precursor, with the filtering and smoothing effect, when the data acquisition system works at a

relative low sampling rate. As Ref. [9] described, the modal wave is a phenomenon characterized by low-frequency low-amplitude pressure wave cover the whole circumferential scale. So, the modal order should be 1, 2, or other integral numbers, that means there is an integer in the circumferential wave period, while non-integer waveform, such as 1.5, cannot exist. The fluctuation signals include 1 or 2 order component of rotor frequency, if the modal waves exist and do not spread in the relative coordinate system. In fact, the component with rotor frequency can always be found in the pressure signals, either at the steady state far before the stall point, or at the stall state. It because that the fluctuation whatever big or small do exist across the circumferential direction. In other words, absolutely event pressure is impossible. This phenomenon can be explained with the pressure signal P1R60S in Fig. 4. The spectrum of P1R60S at far before stall state (0.0001-0.2048s) is shown in Fig. 4(a), while Fig. 4(b) is at near surge state (9.0501-9.2548s). There is the rotor frequency of 273.4Hz in Fig. 4(a), while 268.6Hz in Fig. 4(b) since the rotor speed changed in the process of test.

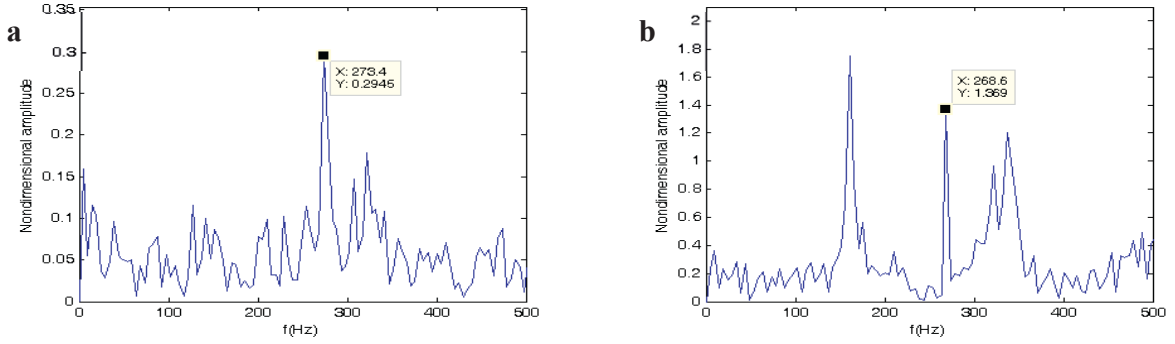

Fig. 4. Spectrums of pressure signal P1R60S,(a) Far before stall; (b) Near surge.

To detect the precursors of instability, the STFT is employed. Usually, the start of surge is defined by the sharply drop point of the outlet total pressure of compressor, followed with fluctuating at large amplitude with low frequency. It is easy to find the start of surge on the time-domain waveform of the outlet total pressure (P7ST), as above mentioned at 9.300s. So, the stall precursors are pursued from the surge point to upwards with the STFT. The pursuit process is explained with the signal P1R60S shown in Fig. 5(a). Generally, the surge or stall frequencies are in the range of 0-300 Hz. In Fig. 5 (a), 0-500 Hz is plotted as interested range. It can be read from Fig. 5 (a) that a band at about 160Hz appears before the surge point (9.300s), which indicates the stall phenomenon. The energy of stall band is larger than the rotor frequency (268.6Hz) component. After the surge point, the energy in focused on a very low frequency band, which again demonstrates that the surge is large-amplitude low-frequency flow vibration.

Fig. 5 (b) is the STFT spectrum of 6.4-6.6s when the analysis window moves upwards from the surge point. The component of 160 Hz and its twice appear in 6.44-6.48s and 6.55-6.58s, which are same as the stall frequencies in Fig. 5 (a). It predicates that the stall precursors present themselves in the two segments. The precursors are

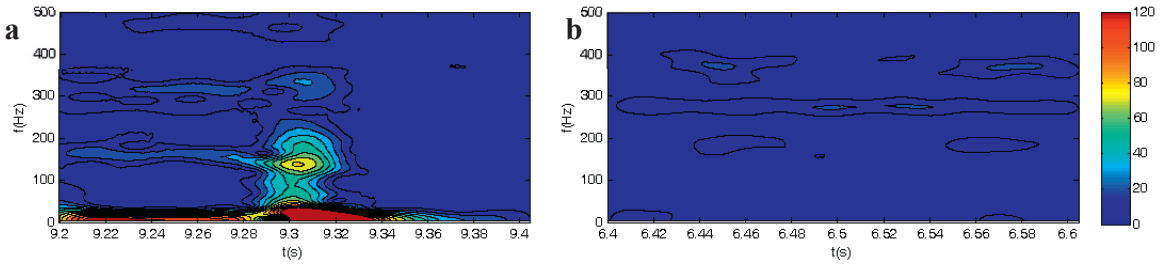

Fig. 5. STFT spectrums of P1R60S, (a) Beginning of surge; (b) Stall precursor.

characterized by appearing intermittent and having near energy with the rotor frequency component.

The same conclusions can be drawn with the others pressure signals, which STFT spectrums are shown in Fig. 6-14. It can determinate that the relative loads of each stage keep balance. So, the stall precursors of each stage occur spontaneously. At the beginning segment, the precursors keep several rotor revolutions. Then, the compressor enters into sustained stall state, while the throttle valve and flow turn down gradually.

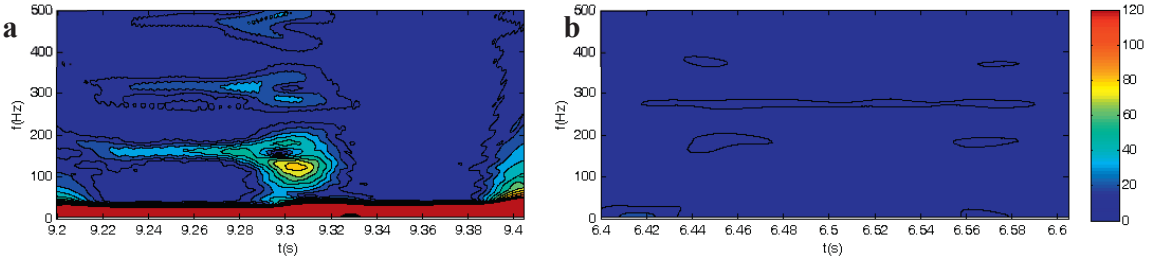

Fig. 6. STFT spectrums of P2R60S, (a) Beginning of surge; (b) Stall precursor.

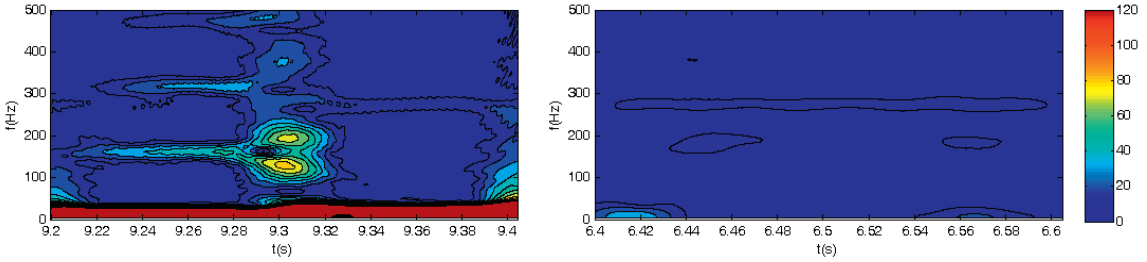

Fig. 7. STFT spectrums ofP2R120S, (a) Beginning of surge; (b) Stall precursor.

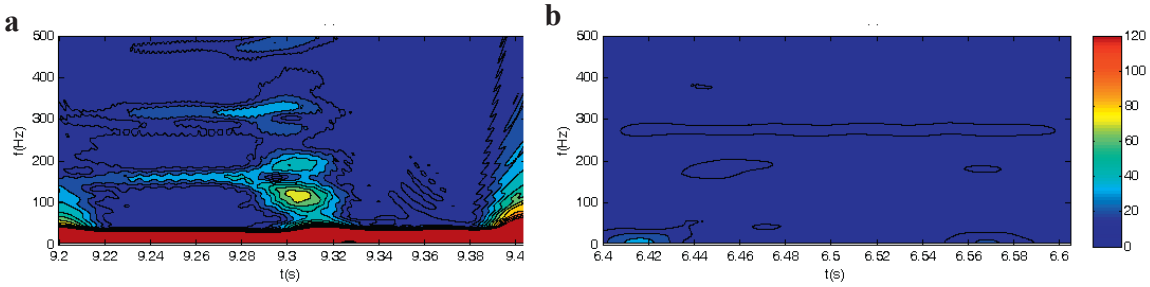

. Fig. 8. STFT spectrums of P3R120S, (a) Beginning of surge; (b) Stall precursor

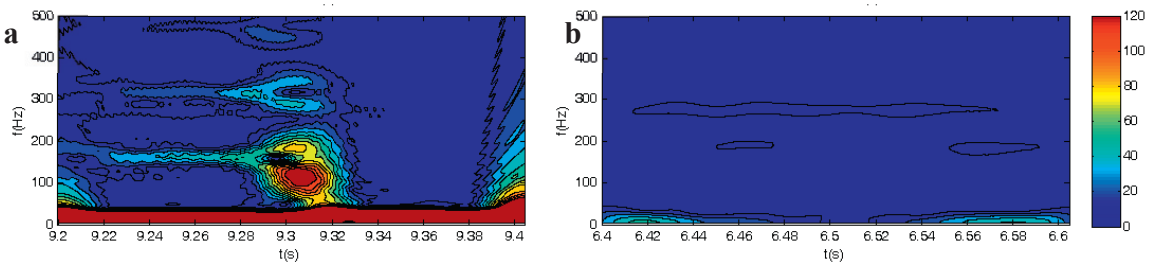

Fig. 9. STFT spectrums of P3S60S, (a) Beginning of surge; (b) Stall precursor.

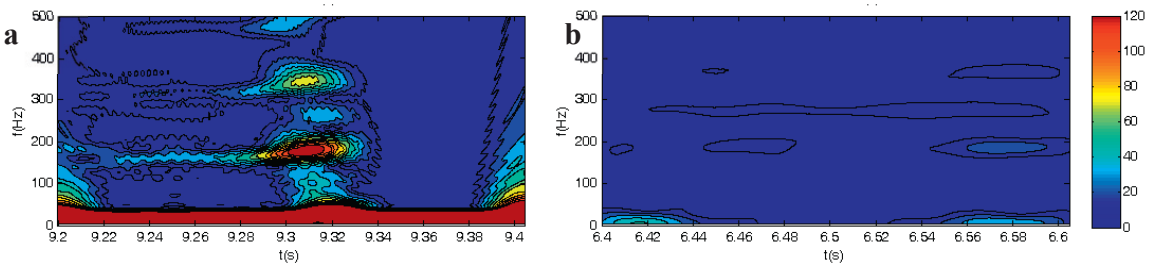

Fig. 10. STFT spectrums ofP4S60S, (a) Beginning of surge; (b) Stall precursor.

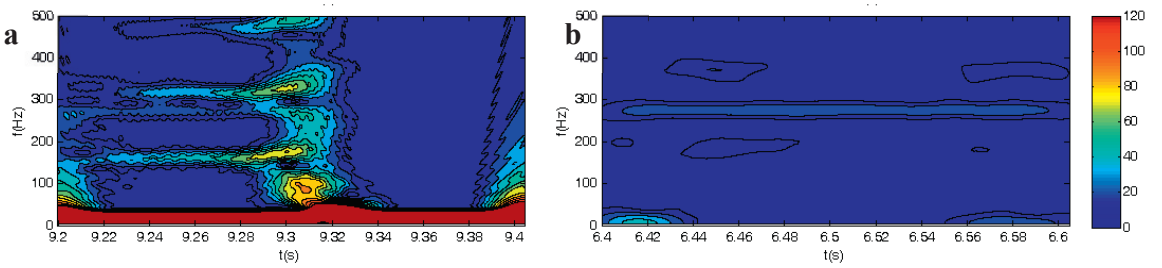

Fig. 11. STFT spectrums of P5R120S, (a) Beginning of surge; (b) Stall precursor.

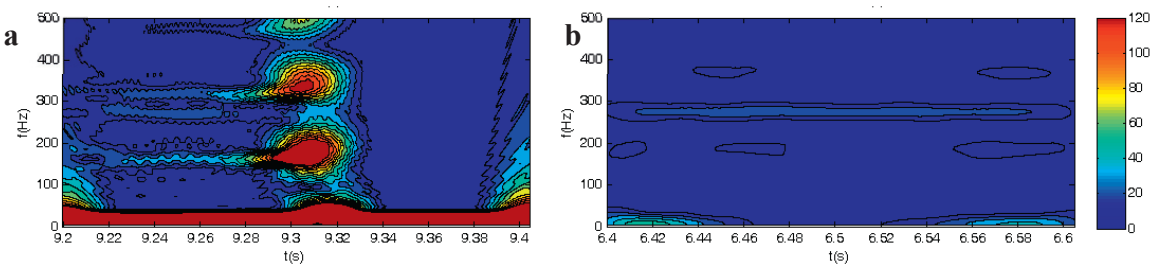

Fig. 12. STFT spectrums of P5S60S, (a) Beginning of surge; (b) Stall precursor.

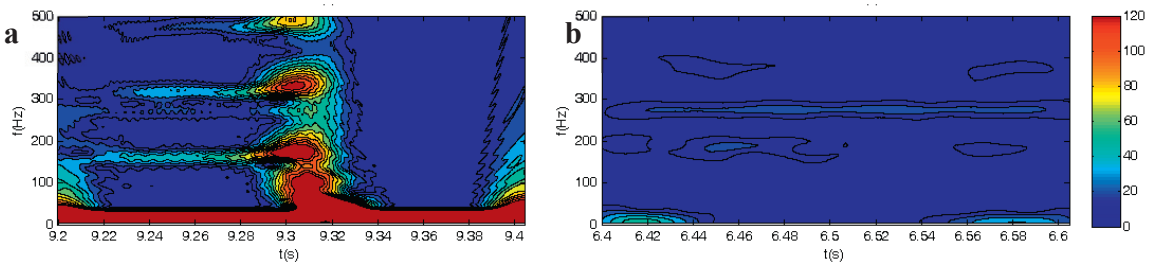

Fig. 13. STFT spectrums of P6R120S, (a) Beginning of surge; (b) Stall precursor.

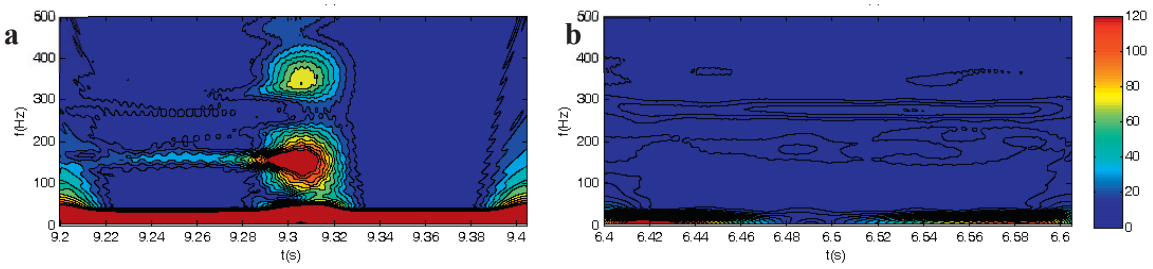

Fig. 14. STFT spectrums of P7R60S, (a) Beginning of surge; (b) Stall precursor.

The time relationships of stall cells spread in the compressor are analysis by the correlation function calculated on signals 9.2000-9.3000s. Fig. 16 shows the correlation function of P1R60S and P2R60S. The stall cell of P2R60S is 0.0002s later than that of P1R60S. There are 0.0064s or 156.25 Hz periods existing in the correlation diagram, which is the frequency of stall cells. So, the stall cells in the second stage have same frequency as the cells in the first stage, namely 156.25 Hz, but they are 0.0002s, or 11.25 degrees (2/64*360) in angles, later.

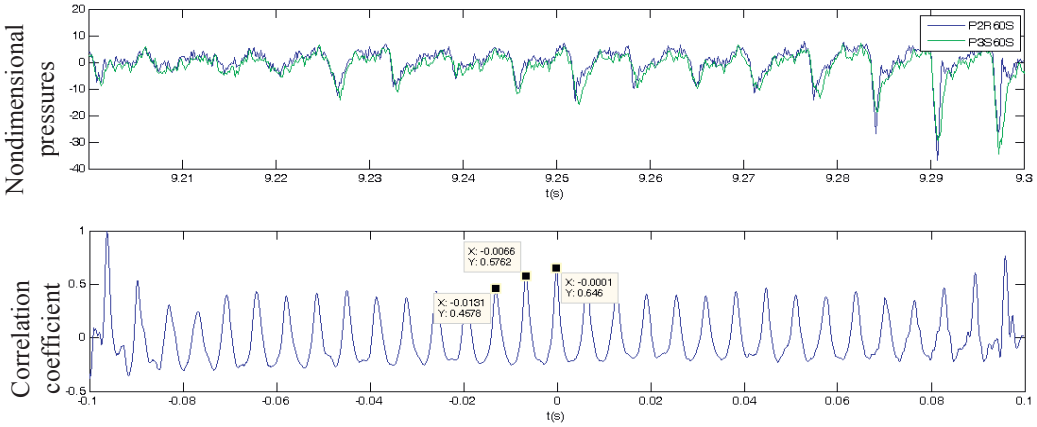

Fig. 15. Cross-correlation function of P3S60S and P2R60S.

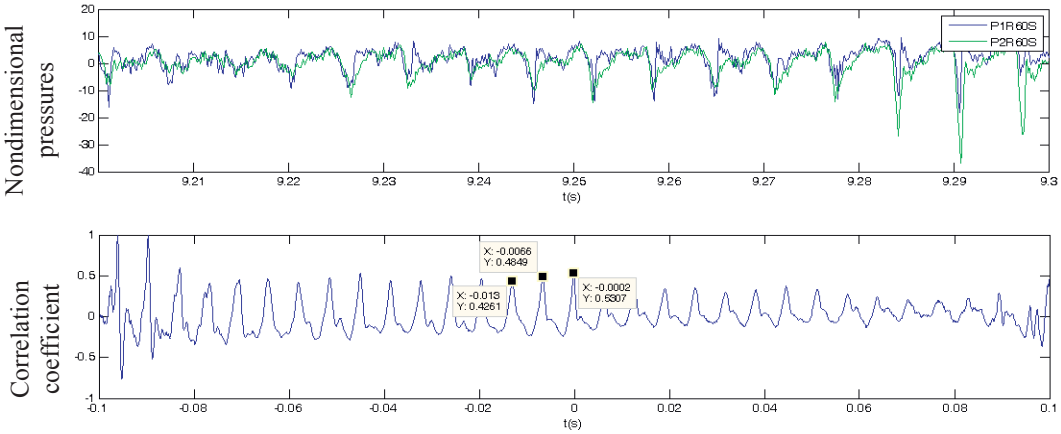

Fig. 16. Cross-correlation function of P2R60S and P1R60S.

The correlation function of P2R60S and P3S60S is shown in Fig. 15. There are 0.0065s or 153.85 Hz periods existing in the figure. The stall cells in the stator of the third stage are 0.0001s, or 5.54 degrees (1/65*360) in angles, later than that in the rotor of the second stage. Finally, the stall cells relative position of every two stages can be calculated by correlation functions and then drown in Fig. 17.

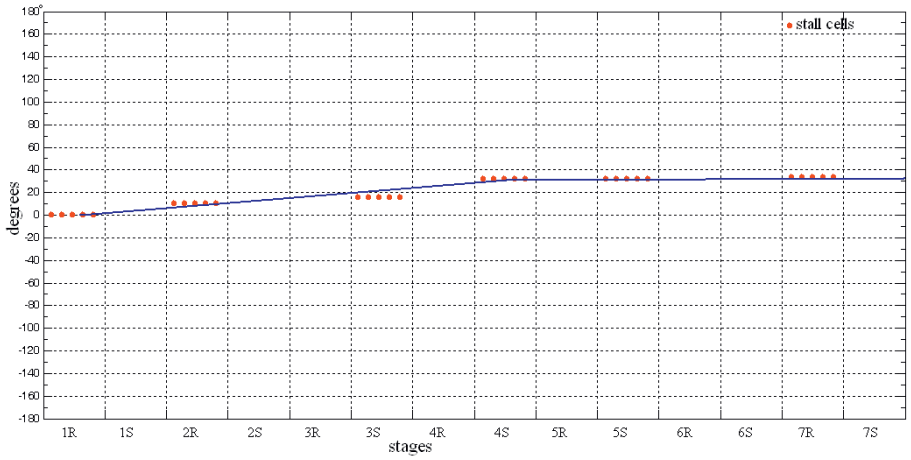

Fig. 17. Relative position of stall cells in each stage.

4.3. Compressor surge process

The Fig. 18 gives the pressure fluctuation process of surge. The S1 is the starting segment of surge process. Fig. 19 give the enlarged figure of the S1 of 9.3000-9.3200s signals of static pressures in the case wall on 60 degree positions, about 5-6 rotor revolutions. The first period of pressure fluctuation is 0.0058s, and the second is 0.253s. Meanwhile, the rotor speed is 16066rpm, or 0.0037s as period. The pressure fluctuation periods are longer than the rotor period, with large amplitude, which is caused by surge. As shown in the red rectangle of Fig. 19, at the starting point T1, the static pressures of P1R60S, P2R60S and P3S60S are raising, while the pressures of P4S60S, P5S60S and P7R60S are decreasing. It means that a stagnant cell occurs after the stator blades of the 3rd stage and before the stator blades of the 4th stage. The stagnant cell pushes the static pressures before it up by slowing down the flow velocity. The static pressures after the stagnant cell decrease because blades add less energy to the flow. At T2 in Fig. 19, the cell moves to the position after the stator blades of the 5th stage, this raised the P5S60S. At T3, the stagnant cell is exhausted from the outlet of the compressor. The velocity of flow rises up drawing the static pressure P7R60S lower. At T4, the flow velocity increases due to the restoring of circulation ability, which makes all static pressures go in downward trend. At T5, a new stagnant cell is born between the stator blades of the 3rdstage and the 4thstage. The P1R60, P2R60S and P3S60S rise up while P4S60S, P5S60S and P7R60S decrease again. Then the cell move backward and exhaust from the outlet of the compressor during T5-T6.

The fluctuation of surge is so strong that exceeding the pre-set measurement ranges of static pressures, resulting in a clipping phenomenon of signals as showing in Fig. 18-19. The outlet total pressure P7ST keeps decreasing throughout the initial section of surge. It suggests that the fluctuation flow with stagnant cells which is found by static pressures on the case wall, are different from the mainstream area of the compressor, and the surge occurs in the tip region and spread to the hub.

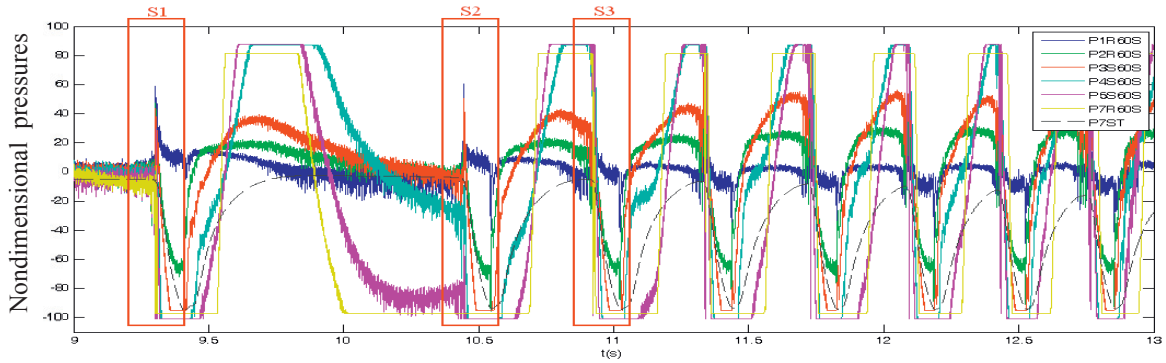

Fig. 18. Pressure signals of surge process.

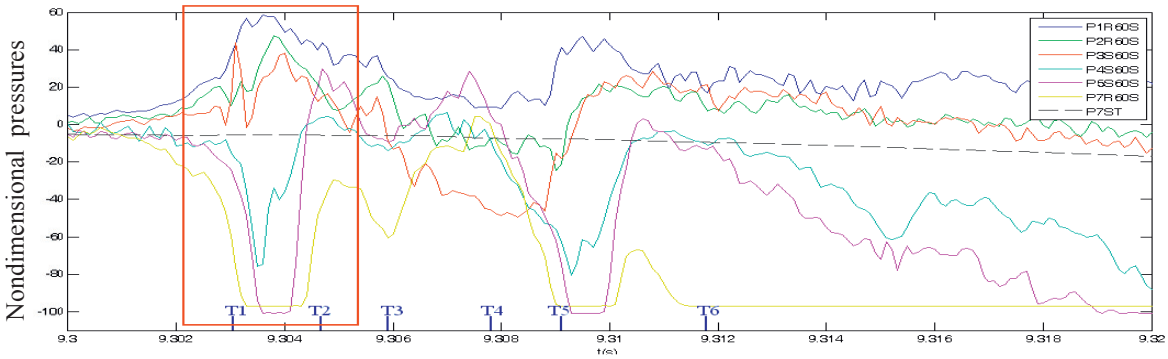

Fig. 19. Beginning segment of surge.

Similar phenomena exist with the S2 and S3 of S1 segment in Fig. 18 that a surge cycle starts by the raising of P1R60S, P2R60S and P3S60S. The difference is that the flow does not return to a steady state at the end of a surge cycle. The enlarged S3 shown in Fig. 21 explains this phenomenon. The flow fields of the 1st to 3rd stages are basically recovered before 10.920s, while the 4th to 7th stages are not. A new surge cycle starts by the marker of the P1R60S, P2R60S and P3S60S raising in 10.920-10.925s.

A whole cycle of the surge process is shown in Fig. 20. As mentioned before, a cycle is started at T1. The stagnant cell of the latest cycle is not exhausted from the outlet at the moment. So, the P4S60S、P5S60S and P7R60S are still higher. The new cell and the old cell move are moving downwards, making casing static pressures lower. The whole flow field of the compressor is worse, and less power adds to the airflow by blades. It leads to lower total pressure of the outlet. The old cell is exhausted from the outlet at T3. Then, the casing static pressures and the total pressure are recovering at T4. The new cell reaches at the last few stage of the compressor, and the flow fields of front stages are basically recovered at T5. At T6, the stall cells are appeared in the front stages. Then, a new cell with low axial velocity occurs, and the new cycle is coming at T7. In the Fig. 21, the surge cycle is 0.4117s, about 110 rotor revolutions.

As mentioned in last paragraph, the front 1stto 3rdstages are the cycle of stall-surge-recover-stall. The fluctuation occurs not only in axial direction, but also in circumferential direction. The autocorrelation function is calculated to find the periodic components of P1R60S, P2R60S and P3S60S in the stall section. The stall frequency of 158.7 is detected. For the latter stages, the main feature is the velocity fluctuates largely in axial direction. Meanwhile, it companies with the stall cells rotating in circumferential direction. This phenomenon can be found with circumferential located sensors such as P5S60S and P5R120S.

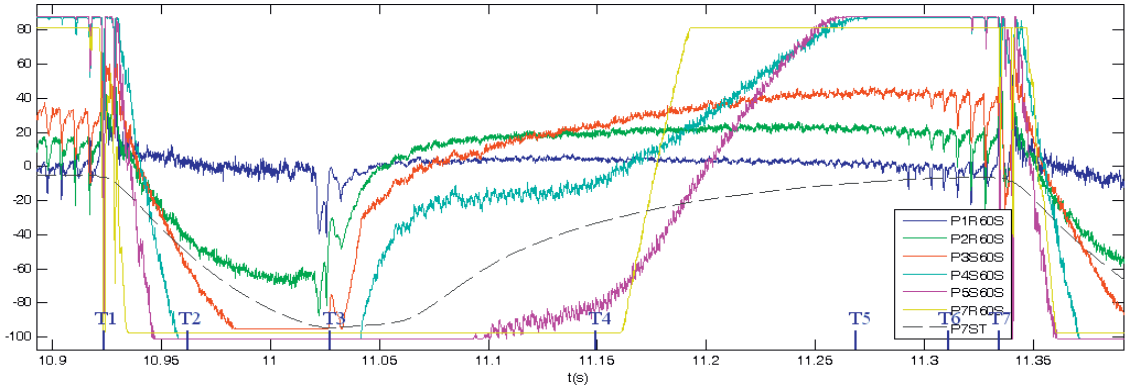

Fig. 20. A whole cycle of the surge process.

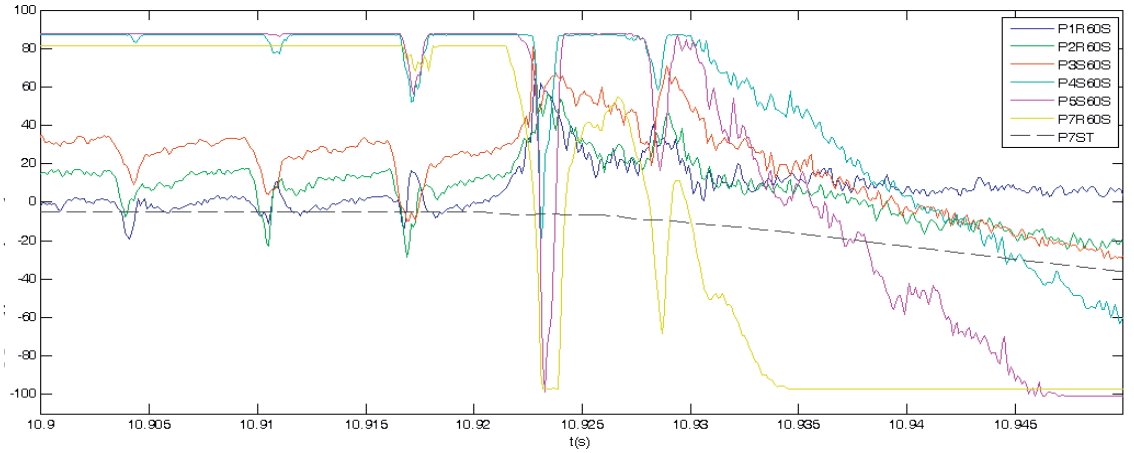

Fig. 21. New cycle of surge.

5. Conclusions

A high-speed seven-stage compressor was examined on the test rig to get the surge boundary and instability signals, with 10 casing static pressure and an outlet total pressure. In this paper, the characteristics and relationships of pressures are analyzed with the case of rotor speed at 16,400RPM.

With the STFT, it is found that the stall precursors appear individually in each stages ~3.5s before the surge, suggesting common stability conditions among all the stages at this speed. It also means that stalls in all or a few stages may not lead to surge directly. It may stay on the stall situation for a not very short time.

The phase or contextual relationships are calculated with the correlation functions. It shows that the rotating stalls of the 1-3 stages have phase differences, while the 4 -7 stages do not.

The casing pressures traces are analysis in detail. The stagnation cell of surge is firstly formed between the 3rd and the 4th stator rows, and then moves downwards. The front 3 stages are in the cycles of the stall-surge-recover-stall in the whole surge process, i.e. the surge is companied with stalls in this compressor.

Acknowledgements

This project is supported by National Natural Science Foundation of China (NSFC) with Grant No. 51205311.

References

[1] N. Courtiade, X. Ottavy, Experimental study of surge precursors in high-speed multistage compressor, ASEM Journal of Turbomachinery ASME. 135(2013) 061018.
[2] G. Pullan, A.M. Young, I. J. Day, et al, Origins and structure of spike-type rotating stall, Proceeding of ASME Turbo Expo 2012, June 11-15, 2012, Copenhagen, Denmark, GT2012-68707.
[3] L. G. N. Bennett, W. D. E. Allan, Examination of rotating stall inception in a small high speed axial compressor, Proceeding of ASME Turbo Expo 2009: Power for Land, Sea and Air, June 8-12, 2009, Orlando, Florida, USA. GT2009-59420.
[4] Y. Wu, F. Dong, J. Lv, et al, Largest Lyapunov exponents of engine experimental data, Chinese Journal of Applied Mechanics, 1(2006) 68-71.
[5] M. Stobel, S. Bindl, R. Niehuis, Rotating stall inception inside the low pressure compressor of a twin-spool turbofan engine, Proceeding of ASME Turbo Expo 2013: Turbine Technical Conference and Exposition, June 3-7, 2013, San Antonio, Texas, USA, GT2013-94220.
[6] K. Yamada, H. Kikuta, K. Iwakiri, et al, An explanation for flow features of spike-type stall inception in an axial compressor rotor, ASME Journal of Turbomachinery, 135(2013) 021023.
[7] J. D. Cameron, S. C. Morris, Analysis of axial compressor stall inception using unsteady casing pressure measurements, ASME Journal of Turbomachinery, 135(2013) 021036.
[8] C. Li, W. Han, B. Xiong, Pattern recognition and on-line detection for compressor surge, Journal of Propulsion Technology, 3(2011) 318-322.
[9] H. D. Vo, Control of rotating stall in axial compressors using plasma actuators, 37th AIAA Fluid Dynamic Conference and Exhibit, June 25-28, 2007, Miami, FL, AIAA 2007-3845.